J. Physiol. (1981), **318**, *pp.* 479–500
With 13 *text-figures*
Printed in Great Britain

SODIUM CURRENT IN SINGLE RAT HEART MUSCLE CELLS

BY A. M. BROWN, K. S. LEE* AND T. POWELL†

From the Department of Physiology and Biophysics, University of Texas Medical Branch, Galveston, TX 77550, U.S.A. and the †Department of Physics as Applied to Medicine, Middlesex Hospital Medical School, London W1P 6DB

(*Received 3 July 1980*)

SUMMARY

1. Rapid inward Na current (I_{Na}) was studied in isolated cells from rat ventricular myocardium by a double-suction-pipette voltage-clamp technique. All experiments were carried out at 20–22 °C.

2. I_{Na} elicited by single depolarizing voltage steps from a holding potential, V_H, of −80 mV had a threshold between −70 and −60 mV and was maximal at −30 to −20 mV. Peak currents in Krebs–Ringer solution containing 145 mM Na were of the order 0·9–1·8 mA cm^{-2}, assuming an average cell surface area of 8000 μm^2.

3. The reversal potential for I_{Na} was predicted by the Nernst equation for external Na in the range 1·45–145 mM, with 16 mM-Na solution perfusing the interior of the cell.

4. Instantaneous I–V plots were linear for potentials of −100 to +10 mV. Maximum Na conductance ($\bar{g}_{Na}$) was calculated to be 25 mS cm^{-2} in 145 mM-Na solutions and g_{Na} was constant for potentials positive to −10 mV.

5. I_{Na} activated with a time constant of 0·7 msec at −55 mV, decreasing to 100 μsec on depolarizations positive to +10 mV.

6. Two time constants (τ_{h_1}, τ_{h_2}) were required to describe I_{Na} inactivation during a maintained depolarization, with τ_{h_2} three to four times as long as τ_{h_1}. τ_{h_1} was about 2 msec at −50 mV, decreasing to 0·9 msec at −10 mV.

7. The time course for recovery of I_{Na} from inactivation also exhibited two time constants (τ_{r_1}, τ_{r_2}), with the longer τ_{r_2} having a maximum value of the order 100 msec in the potential range −60 to −80 mV.

8. I_{Na} in isolated rat cardiac cells has a low sensitivity to tetrodotoxin, requiring a concentration of 30 μM for complete blockade.

INTRODUCTION

In the preceding paper (Brown, Lee & Powell, 1981) a double-suction-pipette technique was described for recording trans-sarcolemmal currents carried by sodium ions, during voltage clamp of individual muscle cells isolated enzymically from adult rat ventricular myocardium. The improved voltage-clamp procedure permits direct analysis of Na currents, measured in cells bathed in solutions containing physiological

* Present address: Department of Physiology, Yale University, New Haven, Connecticut, U.S.A.

concentrations of Na (145 mM) at 20–22 °C. We report here experiments aimed at characterizing both the magnitude of the Na conductance and its kinetics during step changes in potential applied to isolated ventricular myocytes. Although the results can be interpreted in general terms using the Hodgkin–Huxley formulation for squid giant axon (Hodgkin & Huxley, 1952*a–d*), it is shown that the kinetics of Na currents in heart cells are more complex, with the time course of recovery from and development of inactivation exhibiting two exponential components. A modification of the Hodgkin–Huxley scheme which does produce multi-exponential inactivation is a three-state inactivation model, involving one open and two closed states of the inactivation gate in linear sequence (Chiu, 1977) and this was used for part of the data analysis mainly by virtue of its simplicity. Experimental values for the longer time constant for recovery from inactivation at potentials near the resting membrane potential are consistent with the slow time course of Na current recovery reported for multicellular cardiac preparations.

Some of the results on reactivation of the Na conductance have appeared previously in abstract form (Brown, Lee & Powell, 1980).

METHODS

Methods for cell isolation, voltage clamping of single cells with two suction pipettes and data acquisition were as described in the preceding paper (Brown *et al.* 1981). Fast Na current was isolated by using an external solution containing 145 mM-Na, with K and Cl replaced by Cs and isethionate (see Table 1 of Brown *et al.* 1981). Low Na solutions were prepared with isosmotic sucrose replacement or Tris substitution. Ca was omitted or replaced by Mn in some experiments. Internally, the cell was perfused with K-free, Cl-free solutions containing equimolar Cs, aspartate (or fluoride) and 16 mM-Na. For solutions containing tetrodotoxin (TTX), 1 mg of TTX powder (Sigma) was dissolved in 10 ml. distilled water to make an 8×10^{-4} M stock solution, which was then added to the test solution to give the final desired concentration. All experiments were carried out at room temperature (20–22 °C). Currents and voltages were digitized as described previously (Brown *et al.* 1981) and linear components of capacitative and leakage currents were removed by subtraction. Kinetic parameters were measured by hand from semilogarithmic plots or by a curve-fitting programme on a PDP 11/70 computer, using a Fortran version of the pattern-search least-squares estimates for non-linear models (Colquhoun, 1971), kindly provided to us by Dr D. C. Eaton.

RESULTS

Fig. 1*A* shows current–time records (uncorrected for capacitative and leakage currents) obtained during voltage clamp of an isolated cell in an essentially Ca-free solution containing 50 % Na (i.e. half the normal Na concentration of 145 mM). The currents were both time- and voltage-dependent, had a threshold between −70 and −60 mV and increased in magnitude in the inward direction as the potential became more positive, reaching peak amplitude at potentials in the range −30 to −20 mV. Further depolarization reduced the membrane current, until at about +25 to +35 mV the current changed sign to become outward at more positive potentials. Fig. 1*B* shows five currents during their first 1·5 msec, after correction for linear capacity and leakage currents. All records were sigmoidal in shape, with outward currents showing less curvature at more positive potentials. Net currents were preceded by a delay, which was of the order of 100 μsec duration. Without the subtraction procedure, this delay is the period during which capacity current is observed in the current records (Brown *et al.* 1981).

When peak current in 50 % Na is plotted as a function of clamp potential (Fig. 2*A*) the *I–V* curve is not completely symmetrical about the potential producing maximum current, but is steeper at potentials negative to this value than for positive potentials, although in other cells this was not as marked. The maximum peak inward currents recorded in 50 % Na were in the range 35–50 nA, whereas in 100 % Na solutions these

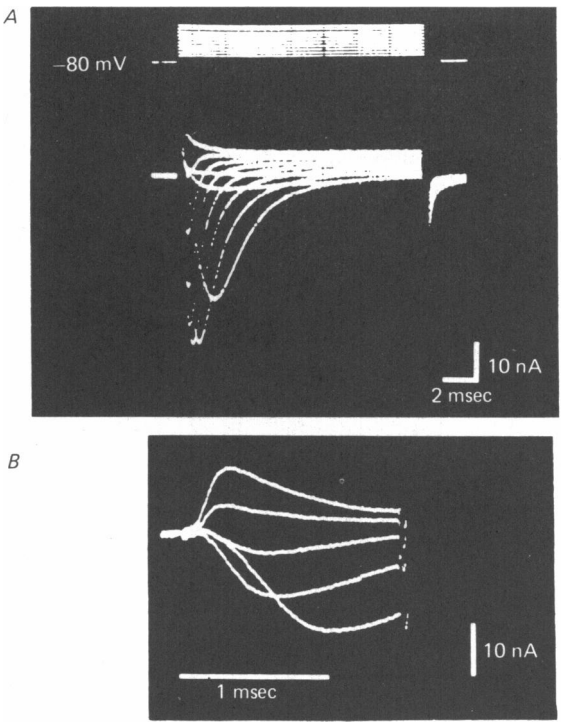

Fig. 1. *A*, sodium currents (lower traces) recorded from a single heart cell under voltage clamp with two suction pipettes. Currents were recorded in Ca-, K-, Cl-free external and internal solutions with 72·5 mM-Na_o (50 %) and 16 mM-Na_i. Holding potential, (V_H) was −80 mV and voltage traces (top) represent clamped potentials from −60 to +30 mV in 10 mV steps. The currents are not corrected for capacitative or leakage currents. *B*, sodium currents at early times. Linear components of capacitative and leakage currents have been subtracted. $V_H = -80$ mV, and currents were produced at clamped potentials of −10, 0, 10, 30, and 40 mV. A zero-current interval (100 μsec) precedes the appearance of Na currents. This interval was obscured by capacitative current transient in non-subtracted records.

currents increased to 70 − 140 nA (Fig. 2*B*). Peak inward currents of these magnitudes were found in cells which had conventional action potentials, required small steady inward currents to maintain a −80 mV holding potential, had low leakage currents and good long-term stability under voltage-clamp conditions. Other cells, which required large currents to produce a similar resting potential and displayed large leakage currents on depolarization, had maximum inward currents as low as 15–30 nA in 100 % Na, but gave *I–V* profiles which were qualitatively the same shape as those shown here.

Asymmetry of the *I–V* curves might arise from poor voltage control due to significant series-resistance effects, but the data of Fig. 2 make this possibility

unlikely, since the curves for 50 and 100% Na are similar in shape, although markedly different in amplitude. Furthermore, when TTX (7 μM) had been added to reduce peak currents in both 50 and 100% Na solutions, I–V profiles are again comparable in shape and consistent with those obtained in the absence of the toxin (Fig. 2A and B). The similarity of the I–V curves over a tenfold range of maximum inward current is strong evidence against there being a series resistance present in these experiments of sufficient magnitude to compromise good clamp control.

The I–V curves and other voltage-dependent state parameters described in subsequent sections were obtained in Ca-free solutions, containing 2·85 mM-Mg. Ca was omitted both to suppress Ca currents and also to improve the frequency of successful attachment of two suction pipettes to a cell (Brown *et al.* 1981). In a few experiments, 1 mM-Mn was substituted for Ca and appeared to shift these voltage-dependent parameters to more positive voltages, but the effects were not studied systematically.

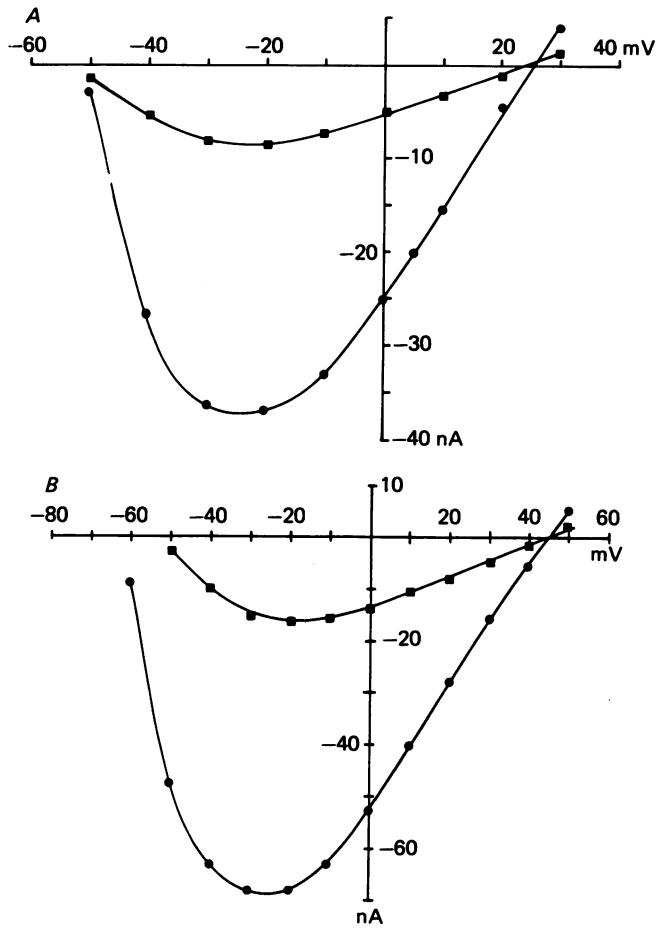

Fig. 2. A, current–voltage relationships of peak I_{Na} in 50% Na_o, ●, and a partially-blocking dose of TTX, ■ (7 μM). The similarity of the I–V curves over a fourfold range of currents indicates that series resistance does not produce significant errors. B, current–voltage relationship of peak I_{Na} in 10% Na_o, ●, and a partially-blocking dose (7 μM) of TTX, ■. The I–V curves differ in scale only.

For cells surviving long enough after suction to permit changes in external solution Na to be made, it was found that currents were reduced as Na was replaced by either sucrose or Tris and that the reversal potential (E_{rev}) was also dependent upon external Na. In solutions containing 100% Na (145 mM), normal Ca (1·1 mM), and Ni (1·0 mM) to block slow inward current, E_{rev} was +56 mV, whereas in 75% Na (110 mM) the reversal potential was +46 mV. When external Na was reduced to 50%

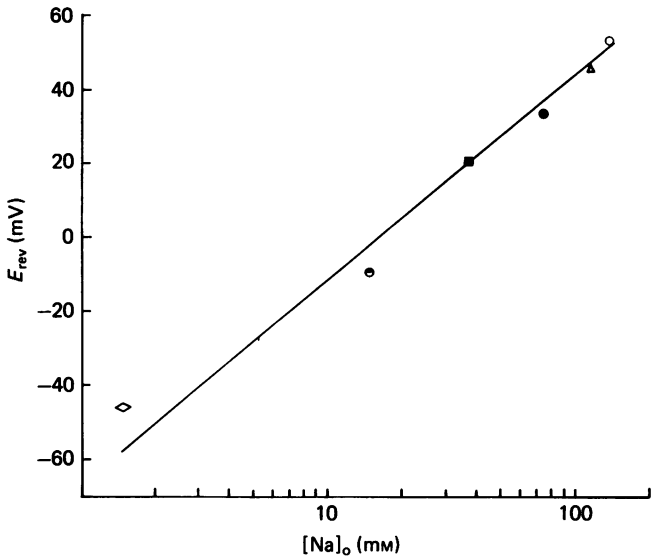

Fig. 3. Effects of changes of $[Na]_o$ on E_{rev}. The continuous line represents the Nernstian relationship. Na concentrations are: 100% (○), 75% (△), 50% (●), 25% (■), 10% (◓) and 1% (◇). 1·1 mM-Ca and 1 mM-Ni were present in the external solution; Ni was used to block slow inward current.

(72·5 mM), 25% (36 mM), 10% (14·5 mM) or 1% (1·45 mM) of the normal value, E_{rev} became +26, +20, −8 and −45 mV, respectively. The experimental values for E_{rev} are consistent with the Nernst relationship of E_{rev} with external Na, calculated at 20–22 °C using an internal Na of 16 mM, assuming equal activity coefficients for Na in both cytoplasm and bathing solution (Fig. 3). The small differences between E_{rev} and E_{Na} in Fig. 3 probably arose from incomplete exchange of internal Na.

These data are all consistent with the hypothesis that the currents measured in the present experiments are due to Na ions passing through Na-specific ionic channels, having voltage- and time-dependent kinetics which are activated during the early phases of membrane depolarization. It will therefore be assumed that these currents are Na currents and they will be given the symbol I_{Na} throughout the remainder of this paper. Scaling of I_{Na} in terms of cell membrane area would enable comparisons to be made with measurements of I_{Na} in other preparations, but it is difficult to make precise determination of the relevant area across which I_{Na} is flowing. Following Page & McAllister (1973) and Powell, Terrar & Twist (1980) it is assumed here that a typical value for cell surface area is of the order of 8000 μm^2, which gives values for membrane electrical constants determined by suction pipettes (Brown *et al.* 1981) which are comparable to those determined by conventional glass micropipettes in both isolated

cells (Powell *et al.* 1980) and whole tissue (Weidmann, 1970). Peak I_{Na} found here of 70–140 nA then corresponds to a peak current density of 0·85–1·75 mA cm^{-2}.

Determination of g_{Na}

Using a classical double-step pulse regime (Hodgkin & Huxley, 1952*b*) and extrapolating I_{Na} back to the beginning of the second step, it was possible to obtain an instantaneous Na I–V curve (Fig. 4) which was linear from −100 mV to about

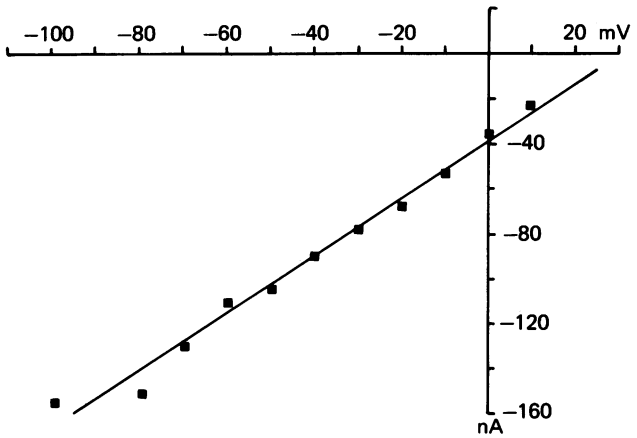

Fig. 4. Instantaneous current–voltage relationship at peak I_{Na}, in 50% extracellular Na. $V_H = -80$ mV. This was determined by stepping the voltage to −20 mV for 200 μsec and then stepping to the potentials indicated on the voltage axis. The tail currents were extrapolated back to zero time and linear components of capacitative and leakage currents were subtracted. The instantaneous curve is linear, as is the ascending limb of the peak I–V curves (Fig. 2).

10 mV negative to E_{Na}. It proved difficult to extrapolate I_{Na} back to the beginning of the second step at voltages nearer the reversal potential, because the activation time constant was approaching the time constant of the capacitative current transient, precluding precise determination of the I–V relationship, The available data indicated a simple ohmic conductance and this is supported by the linearity of the I–V relationship at positive potentials (Fig. 2). Therefore, the Hodgkin–Huxley chord conductance model was assumed in order to calculate g_{Na} from the peak I_{Na} I–V plot. The conductance was related to voltage in a sigmoidal fashion (Fig. 5), with a threshold potential of about −60 mV and a plateau maximum reached at about −10 mV. The plateau region corresponds to the linear portion of the positive slope conductance on the I–V curve and maximal conductance, $\bar{g}_{Na}$, is calculated to be 25 mS cm^{-2} in 100% Na at room temperature, assuming a cell surface area of 8000 μm^2.

Activation of I_{Na}

The time constant for I_{Na} activation (τ_m) at a given potential was determined by three independent methods, all of which gave similar results. In the first method, current–time records from a single voltage-clamp step were inverted, plotted semilogarithmically and the half-time of the initial current rise calculated. Similar

values for τ_m were obtained by measuring the time required to reach peak I_{Na} from the original records and then subtracting the delay which occurred before I_{Na} activation. Thirdly, a curve-fitting algorithm was used on net currents, produced by subtracting the linear components fo capacitative and leakage currents from the original current–time traces (see Methods). This algorithm was based on an m^3h Hodgkin–Huxley model for squid giant axon, in which a small current persists due

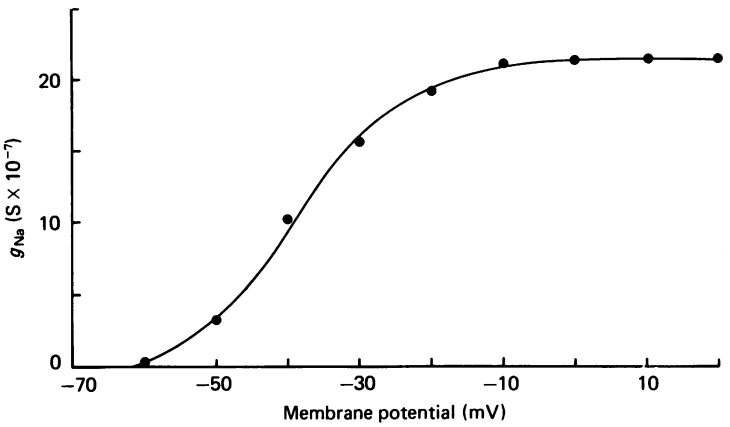

Figs. 5. Relationship between g_{Na} and voltage. g_{Na} was calculated from the chord conductance

$$g_{Na} = \frac{I_{Na}}{V - V_{Na}}$$

g_{Na} showed an e-fold change for a potential change of about 6 mV. Maximum Na conductance, $\bar{g}_{Na}$, in 100 % Na_o was 25 mS cm^{-2}, assuming a cell surface area of 8000 μm^2.

to incomplete inactivation (Meves, 1978). Justification for the algorithm's use comes from the fact that the present I_{Na} was found to inactivate with two time constants, one sufficiently slower than the other so that for a 10 msec voltage-clamp step it could be considered persistent. The curve-fitting routine produced satisfactory fits to the experimental records at these short times (Fig. 6*A*) and the variation of τ_m with membrane potential calculated using this model, which is consistent with the two other methods for estimating τ_m, is shown in Fig. 6*B*. Near threshold, τ_m had values on the order of 0·3 msec (mean, range 0·2–0·4 msec), reaching a maximum of 0·67 msec (mean, range 0·62–0·78 msec) at about −55 mV and then decreasing to approximately 100 μmsec on depolarization to potentials more positive than +10 mV (Table 1).

Inactivation of I_{Na}

The curve-fitting algorithm also allowed estimates to be made of τ_h, the inactivation time constant for I_{Na} (Table 1) during a single voltage clamp step, assuming some persistence of the Na current. With this method, values for τ_h at potentials more negative than the usual holding potentials of −80 to −90 mV could not be obtained. As shown in Fig. 6*C*, τ_h decreased as potentials became more positive than −70 mV, being about 9·2 msec (mean; range 4·7–15·9 msec) at −60 mV and 1 msec at −10 mV. When the values for the relaxation phase of experimental records of I_{Na} were plotted semilogarithmically, however, it appeared that two components were present (Fig.

7*A*). A shorter time constant (τ_{h_1}) dominated for over 90% of the relaxation, but a second time constant (τ_{h_2}) was always observed. This was the reason for adopting a classical Hodgkin–Huxley model, but including incomplete inactivation. When inactivation time constants were plotted as a function of membrane potential (Fig. 7*B*), it was clear that τ_{h_1} was similar in magnitude to the values found for τ_h by curve-fitting and that both differed clearly from the longer τ_{h_2}. For both completion and comparison, the experimental values for τ_m are also included in Fig. 7*B*.

Steady-state inactivation (h_∞) was obtained by investigating the effect of a 40 msec

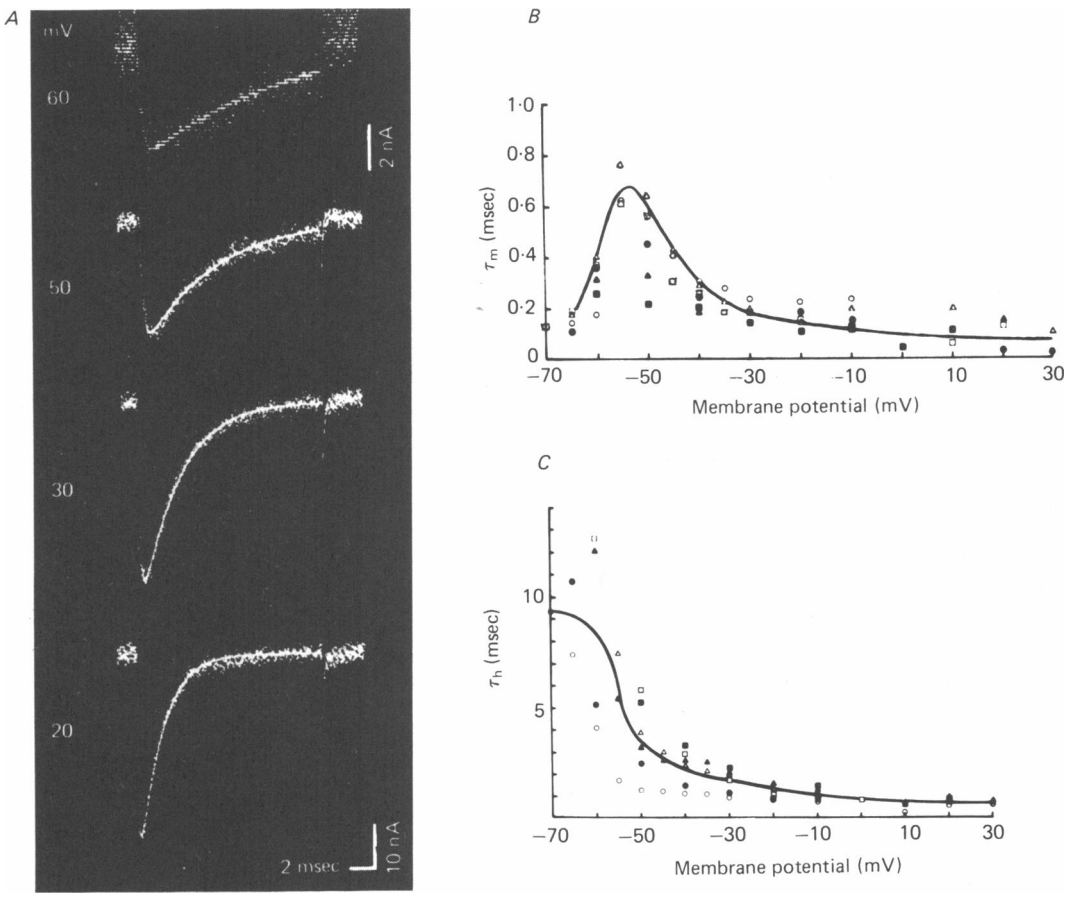

Fig. 6. *A*, Na current traces fitted to an m^3h Hodgkin–Huxley model with incomplete inactivation (persistent current) using a non-linear least-square fitting algorithm, $V_H = -80$ mV. Clamped potentials indicated on the left hand side. Dots are experimental net current time records. Thin lines are the fits. The model fits are satisfactory, although it is possible to fit inactivation with two time constants, as Fig. 7*A* suggests. *B*. relationship between activation time constant, (τ_m), and voltage. Each symbol represents a different experiment. At −65 mV, τ_m had an average of about 0·17 msec, which increased to 0·67 msec at −55 mV and decreased to 0·1 msec at +10 mV membrane potential. Continuous line drawn by eye. *C*, relationship between inactivation time constant, τ_h, and membrane potential. Same set of experiments as shown in Fig. 6*A*. τ_h has mean value of 9·2 msec at membrane potential of −60 mV, decreasing to 1 msec at −10 mV membrane potential. Line drawn through mean values by eye.

prepulse on the current produced by a test pulse to −20 mV of identical duration (Fig. 8*A*). As the prepulse potential became more positive, the test pulse current was reduced. The ratio of current amplitude with prepulse to that without prepulse is plotted against prepulse potential in Fig. 8*A* and affords a measure of h_∞. The experimental data could be fitted by an equation of the form

$$h_\infty = \frac{1}{(1+\exp(V-V_h)/k)}$$

(Hodgkin & Huxley, 1952*c*), where the half-inactivation voltage (V_h) was at −66 mV and the slope factor (k) was 11 mV. At −80 mV, h_∞ is 0·8.

TABLE 1. Potential dependence of the time constants of activation, τ_m and inactivation, τ_h

E_m (mV)	τ_m (msec) mean	± S.D.	n	τ_h (msec) mean	± S.D.	n
−70	0·13	—	1	9·4	—	1
−65	0·17	0·03	4	8·4	2·3	2
−60	0·32	0·08	6	9·2	4·4	4
−55	0·67	0·08	3	4·8	2·9	3
−50	0·46	0·16	6	3·7	1·7	6
−45	0·38	0·06	3	3·2	1·6	3
−40	0·25	0·05	6	2·3	0·9	6
−35	0·23	0·05	3	1·9	0·7	3
−30	0·19	0·03	4	1·7	0·5	5
−20	0·18	0·05	5	1·2	0·3	4
−10	0·16	0·05	5	1·1	0·2	5
0	0·14	0·04	2	0·8	0·02	2
+10	0·12	0·08	3	0·7	0·23	3
+20	0·11	0·05	3	0·68	0·16	3
+30	0·10	0·05	2	0·65	0·14	2

Data obtained from six cells. Values were calculated from a computer fit to an m^3h Hodgkin-Huxley model with persistent current (see text). Note that the number of values at each voltage may be less that six because the voltage-clamp records were not complete (cf. Fig. 6*B* and *C*).

Once h_∞ had been determined, the h_∞–V curve could be compared with the curve for steady-state activation of I_{Na} (m_∞). By normalizing the g_{Na} curve shown in Fig. 5 and assuming an m^3h conductance model, although m^4h gave an equally good fit, the dependence of m_∞ on membrane potential was extracted by taking the cube root of the g_{Na}–V relationship (Fig. 8*B*). At about −50 mV, m_∞ was 0·5 and m_∞^3 overlapped h_∞ in the voltage range −70 to −30 mV, an observation which is consistent with the persistence of inward currents within this range of membrane potentials.

Experiments were also undertaken to investigate the time course for the recovery from I_{Na} inactivation and the onset of inactivation using prepulse techniques; these results are considered in the next section.

Recovery of I_{Na}

The time constant for the recovery of I_{Na} from complete inactivation (τ_r) was determined with the pulse sequence shown in Fig. 9*A*, which is a similar paradigm

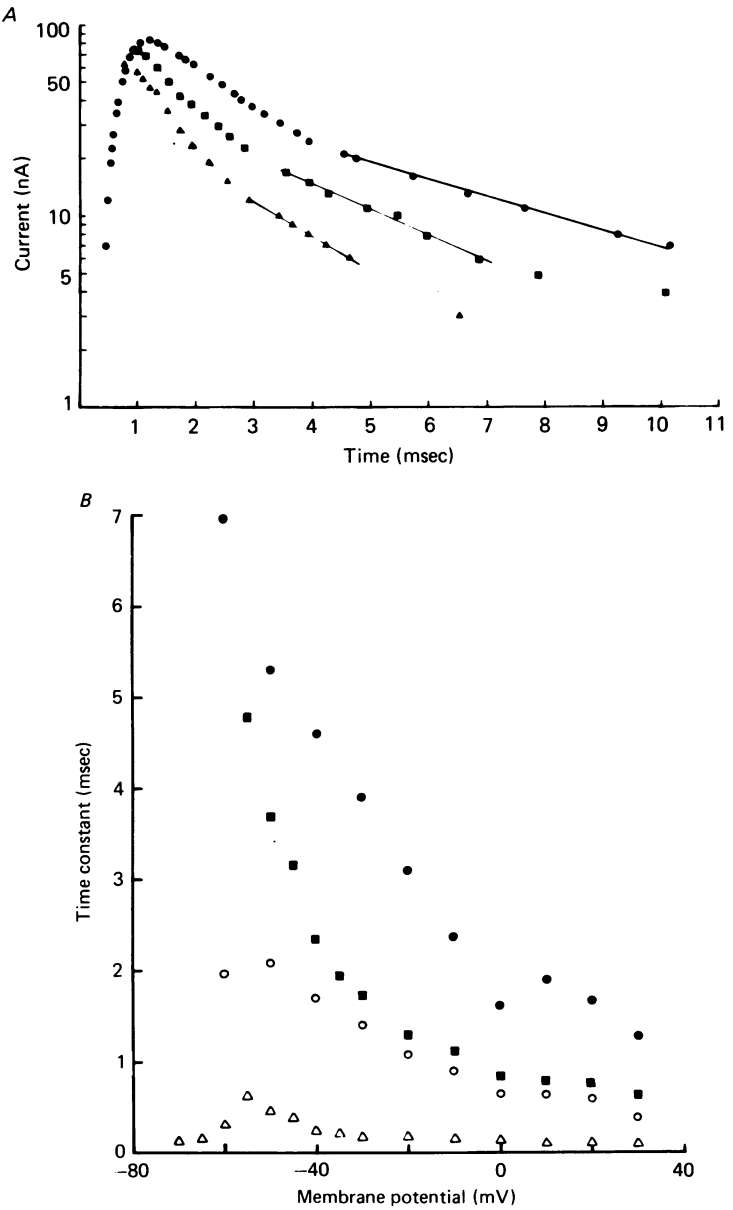

Fig. 7. *A*, three current–time traces produced at potentials of −30 (●), −20 (■) and −10 (▲) mV were inverted and plotted semilogarithmically. Inactivation of the three current traces could be fitted by two exponential functions, and two inactivation time constants, τ_{h_1} and τ_{h_2}, were determined from the half-times of the semilogarithmic plots. τ_{h_1} values were calculated after subtraction of the contribution of the τ_{h_2} component. τ_{h_1} values computed in this manner were slightly smaller than τ_h determined from the computer-fitted traces. *B*, comparison of relationship of τ_{h_1} (○), τ_{h_2} (●), τ_h (■) and τ_m (△) with membrane potential. Computer-extracted τ_h values fell near to τ_{h_1}.

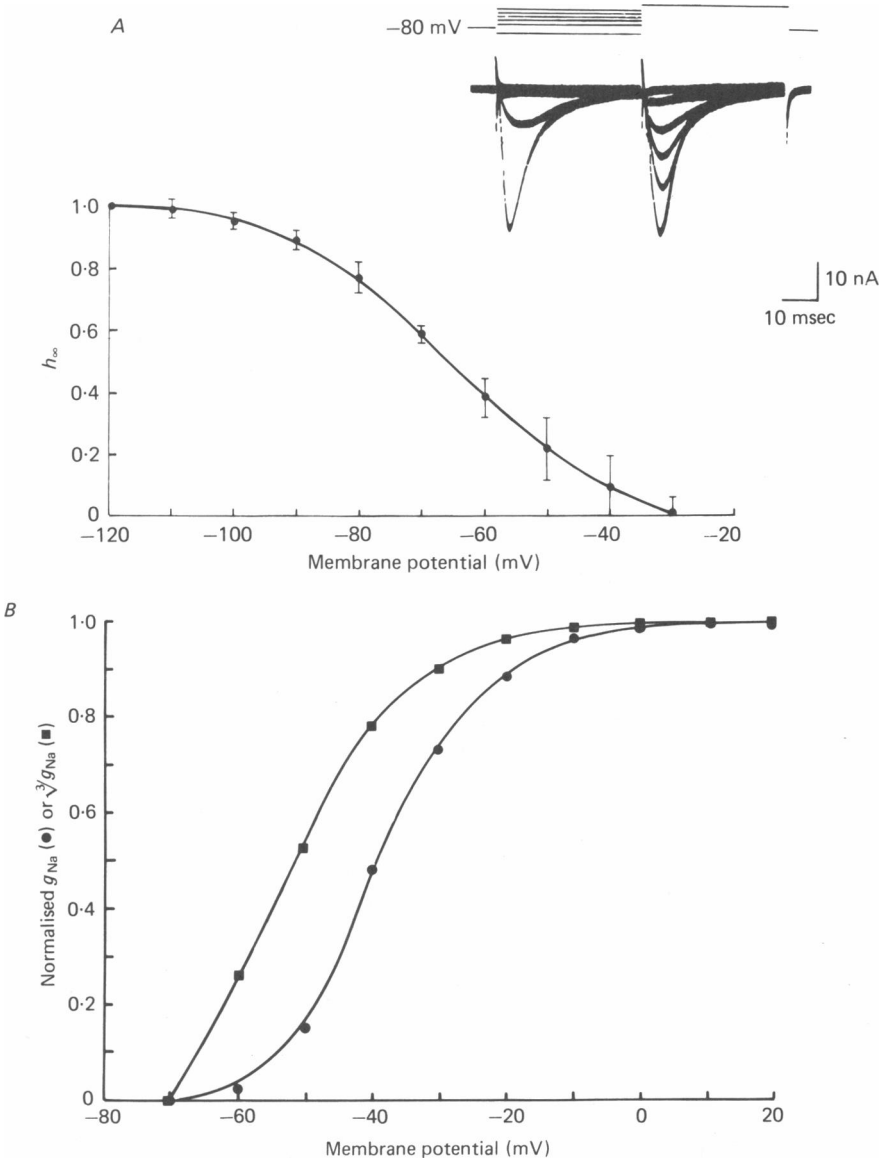

Fig. 8. *A*, relationship of steady-state inactivation, h_∞, and membrane potential, averaged from eleven cells. Inset is the prepulse-test pulse programme, in which the prepulse potential was changed from −100 to −90, −80, −70, −60, −50 and −40 mV, with the test pulse voltage at −30 mV. Currents were not corrected for capacitative or leakage components. Both pulses were 40 msec in duration. The test-pulse current amplitude was expressed as a fraction of the test-pulse current in the absence of a prepulse (ordinate) and was plotted against the corresponding prepulse potential (abscissa). Half-inactivation potential, V_h, was about −66 mV and the curve was fitted to

$$1/(1+(\exp(V-V_h)/k))$$

where k, the slope factor, was calculated to be 11 mV. At holding potential of −80 mV, $h_\infty = 0{\cdot}8$. *B*, steady-state activation of the Na current. m_∞–V curve (■) was obtained by taking the 3rd root of the g_{Na}–V curve (●). h_∞ and m_∞^3 overlapped in the potential range −70 to −30 mV (*cf.* Fig. 8*A*).

to that employed by Haas, Kern, Einwachter & Tarr (1971) in their study of Na-inactivation kinetics in frog atria. Two pulses of 60 mV amplitude and 40 msec duration were used, with the pulse interval varied between 1 and 190 msec. Fig. 9*B* illustrates the current records obtained when the two pulses were initiated from a potential of −80 mV. A test pulse delivered immediately following the prepulse did

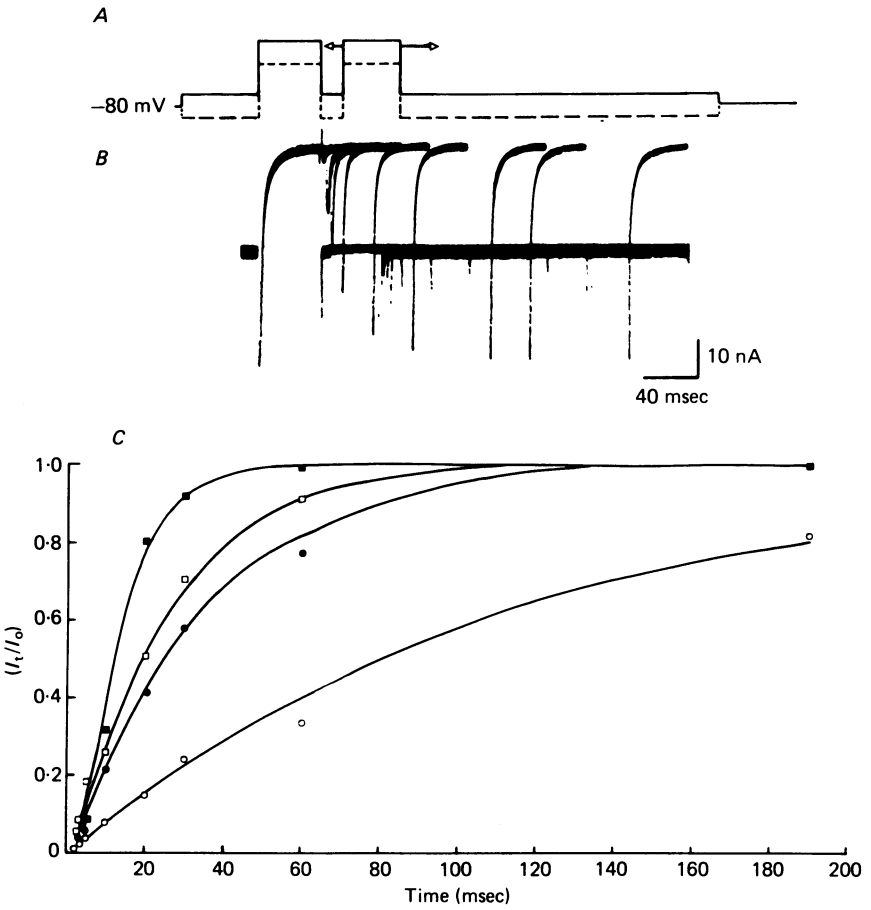

Fig. 9. Time course of recovery of the Na system from complete inactivation. *A*. Pulsing paradigm consisted of a base-line step of 600 msec duration upon which prepulses and test pulses of similar amplitudes and durations (60 mV, 40 msec) were superimposed. The prepulse occurred 100 msec after the onset of the base-line step. *B*, current records are shown as the time interval between the end of the prepulse and onset of the test pulse was increased from 1 msec to 2, 3, 4, 5, 10, 20, 30, 60 and 190 msec. The base-line step was then changed to a new potential, while the sequence, amplitude and duration of superimposed pre- and test-pulses remained the same. *C*, ordinate: I_t/I_0, where I_t is test-pulse current at time t after end of the prepulse and I_0 is prepulse current. Abscissa: time interval (t, msec) between end of prepulse and onset of test pulse. Each curve represents recovery time course of I_{Na} from inactivation at base-line potentials of −70 (○), −80 (●), −90 (□) and −100 (■) mV. Lines drawn are best fit to experimental points and correspond to two exponential components with time constants τ_{r_1} and τ_{r_2}, which had the values 1·9 and 119 msec (−70 mV), 1·7 and 33 msec (−80 mV), 3·3 and 25 msec (−90 mV), and 3·9 and 10 msec (−100 mV) respectively.

not elicit any current, but as the pulse interval was lengthened a test pulse current appeared and became progressively larger, to finally equal the current amplitude produced by the prepulse. To obtain recovery kinetics at different membrane potentials, the pulse sequence was superimposed on a base-line step from the holding potential and the protocol repeated for base-lines at −100, −90 and −70 mV. The ratio (p) of test pulse to prepulse current amplitude was plotted as a function of interpulse duration for each of the four potentials and representative data are shown in Fig. 9*C*.

The continuous lines in Fig. 9*C* are the best fits to the experimental points calculated using a steepest descent least-squares algorithm (Marquardt, 1963) and the curves are sigmoidal in shape, described by the difference between two exponentials with time constants τ_{r_1} and τ_{r_2} ($\tau_{r_1} < \tau_{r_2}$). A three-state inactivation model, involving one open and two closed states of the Na inactivation gate in linear sequence (Chiu, 1977), predicts such a bi-phasic time course for recovery from

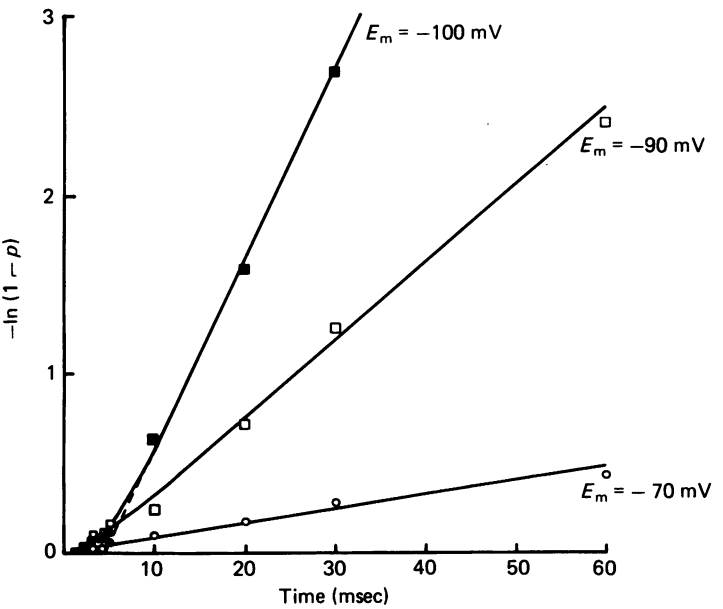

Fig. 10. Data from Fig. 9*C* for −70, −90 and −100 mV plotted semilogarithmically. Ordinate: $-\ln(1-p)$, where $p = (I_t/I_0)$. Abscissa: time (msec) as in Fig. 9*C*. Assuming a three-state inactivation model (Chiu, 1977; eqns. (14) and (15)), the plots should relax finally with straight lines having slopes ($1/\tau_{r_2}$) and intercepts given by

$$\tau_{r_2} \ln\left(\frac{(\tau_{r_2}/\tau_{r_1})}{(\tau_{r_2}/\tau_{r_1})-1}\right).$$

Using linear least-squares analysis, τ_{r_2} was 118 msec with intercept 2·0 msec for −70 mV; 23 msec and intercept 2·9 msec at −90 mV; and 9·5 msec with a 4·4 msec intercept at −100 mV. Values for τ_{r_1} were then calculated to be 2·0 msec (−70 mV), 2·7 msec (−90 mV) and 3·5 msec (−100 mV). In Chiu's model, the amplitudes of the two exponential components are fully determined by τ_{r_1} and τ_{r_2} (Chiu, 1977; eqn. (14)) and calculated values agreed well with those used for the curve-fits in Fig. 9*C*. At −100 mV, the slow component has an amplitude of the order threefold greater than the fast component, whereas at −70 mV this ratio increases to about 60.

complete inactivation and was chosen for further analysis of the data solely by virtue of it being one simple next alternative to the two-state inactivation model of Hodgkin & Huxley (1952*d*), which cannot explain the observations. If the recovery time course was monoexponential, then a plot of $-\ln(1-p)$ against time should yield a straight line passing through the origin. However, plots of this type using the experimental points from Fig. 9*C* show clear deviations from linearity (Fig. 10), with recovery relaxing into a single exponential only at times longer than approximately 2–8 msec. The slope of the line fitted to the late recovery points by standard linear least-squares

TABLE 2. Inactivation time constants for Na current

E_m (mV)	τ_{h_1} (msec)	τ_{c_1} (msec)	τ_{r_1} (msec)	τ_{h_2} (msec)	τ_{c_2} (msec)	τ_{r_2} (msec)
−110	—	4·0±1·8 (3)	8 (1)	—	—	12 (1)
−100	—	3·5±0·7 (3)	5·2±2·0 (3)	—	—	14·7±10·1 (3)
− 90	—	—	4·7±1·9 (5)	—	—	19·6± 8·4 (5)
− 80	—	—	2·1±0·9 (4)	—	—	40·8±13·6 (4)
− 70	—	2·1±0·7 (3)	1·5±0·5 (6)	—	—	90·3±60·4 (6)
− 60	1·9 ±0·2 (4)	1·1±0·5 (3)	—	6·9±2·0 (4)	8·1±1·7 (3)	—
− 50	2·1 ±0·5 (4)	0·7 (1)	—	5·3±1·3 (4)	5·5 (1)	—
− 40	1·7 ±0·2 (4)	0·8±0·2 (3)	—	4·6±0·8 (4)	4·2±2·5 (3)	—
− 30	1·4 ±0·3 (4)	—	—	3·9±1·1 (4)	—	—
− 20	1·1 ±0·1 (4)	—	—	3·1±0·9 (4)	—	—
− 10	0·85±0·05 (4)	—	—	2·3±0·9 (4)	—	—
0	0·63±0·03 (3)	—	—	1·6±0·2 (3)	—	—
+ 10	0·63±0·03 (2)	—	—	1·9±0·5 (2)	—	—
+ 20	0·60±0·03 (2)	—	—	1·7±0·2 (2)	—	—
+ 30	0·4 (1)	—	—	1·3 (1)	—	—

τ_{h_1}, τ_{h_2} values from maintained depolarization (Fig. 1*A*).
τ_{c_1}, τ_{c_2} values from pulse protocol shown in Fig. 11*A*.
τ_{r_1}, τ_{r_2} values from pulse protocol shown in Fig. 9*A*.
Where possible, mean±S.D. has been given, with number of cells in parentheses.

analysis was taken as a measure of the final relaxation time constant (τ_{r_2}) at every potential. Assuming a three-state inactivation model, the intercept of this line with the time axis is a specific function of τ_{r_2} and the ratio τ_{r_2}/τ_{r_1} (Chiu, 1977; eqns. (14) and (15)), permitting calculation of τ_{r_1}. Values for τ_{r_1} and τ_{r_2} found by both curve-fitting the untransformed data (Fig. 9*C*) and analysis of the semilogarithmic plots (Fig. 10) were in good agreement (see legends to both Figures) and are summarized in Table 2. τ_{r_2} was 12 msec (one cell) at −110 mV, increasing to 90·3±60·4 msec (mean±S.D.; six cells) at −70 mV. The data for −70 mV could be divided into two groups, three cells with τ_{r_2} values in the range 30–40 msec and three other cells having much longer recovery time constants in the range 100–170 msec. Values for the faster component (τ_{r_1}) showed a reverse potential dependence compared with τ_{r_2}, with τ_{r_1} decreasing from 8 msec at −110 mV (one cell) to 1·5±0·5 msec (mean±S.D; $n = 6$) at −70 mV. Recovery time constants could not be examined at potentials more positive than −70 mV with this protocol, because the currents were too small.

In an attempt to bridge the potential range over which τ_{r_1} and τ_{r_2} were measured with that used for τ_{h_1} and τ_{h_2}, the onset of inactivation or recovery of I_{Na} was estimated in a separate set of experiments using a variable duration prepulse (0·2–8 msec) in the range −40 to −110 mV, followed immediately by a test pulse

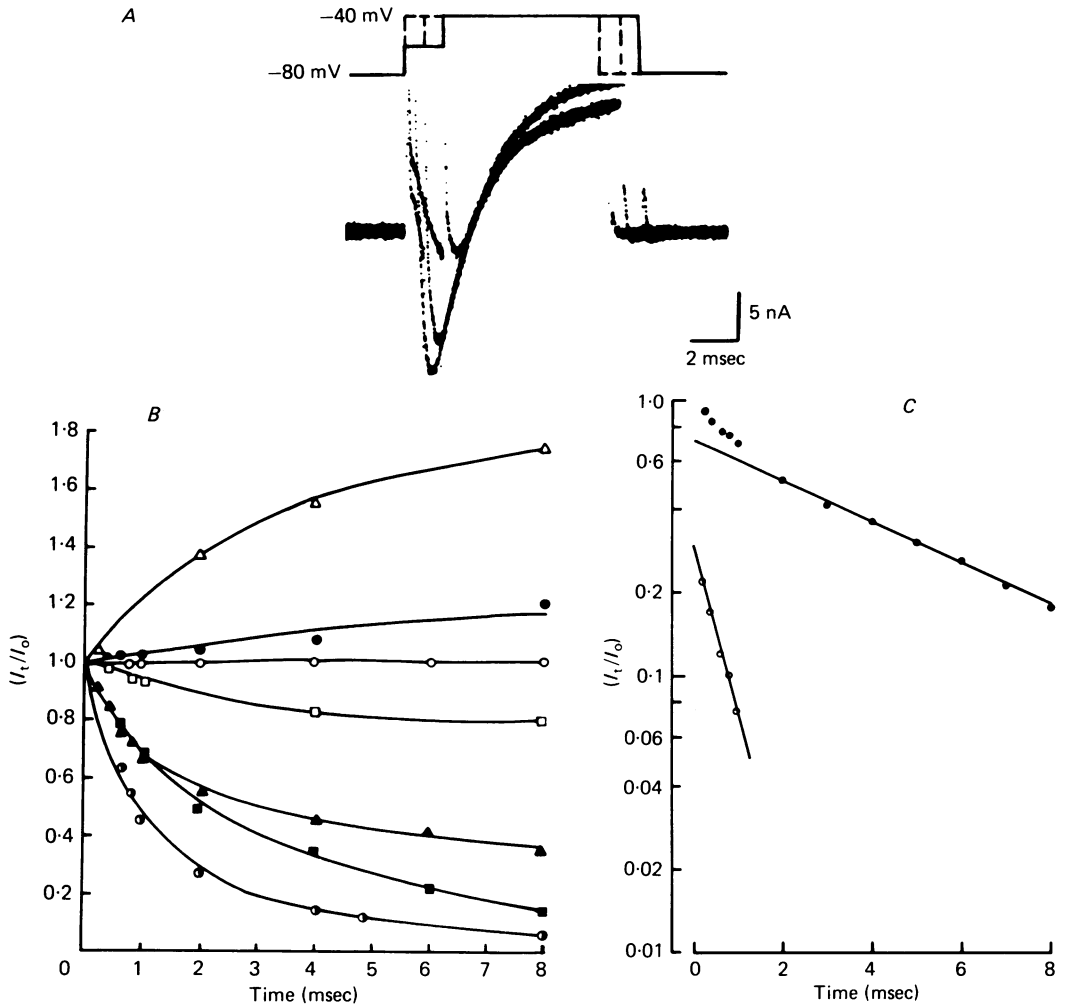

Fig. 11. Onset of inactivation and recovery from inactivation measured by prepulse effects on test pulse current amplitude. *A*, pulse programme and resulting Na currents. At a fixed prepulse potential, the duration of the prepulse was increased from 0·2 msec to 0·4, 0·8, 1, 2, 4, 6 and 8 msec. The test pulse potential and duration was constant at −30 mV and 20 msec. Holding potential (V_H) was −80 mV. *B*, ordinate: (I_t/I_o), where I_t is the test-pulse current amplitude following a prepulse of duration t msec, and I_o is the test-pulse current produced without prepulse. Abscissa: duration of prepulse (msec). Prepulse potentials were −40 (◑), −50 (■), −60 (▲) and −70 (□) mV for measurements of onset of inactivation, and −90 (○), −100 (●) and −110 (△) mV for recovery experiments. The curves for −40, −50 and −60 mV could be fitted by the sum of two exponentials (see below), whereas at all potentials negative to this range only one exponential was required. This was due to the fact that prepulses were used only to a maximum duration of 8 msec (see text). *C*, data for prepulse potential of −50 mV shown in Fig. 11*B* plotted semilogarithmically. Ordinate: $(I_t/I_o) = p$. Abscissa: duration of prepulse (msec). In general, curves could be fitted by an equation of the form

$$p(t) = p(\infty) + A \exp(-t/\tau_{c_1}) + B \exp(-t/\tau_{c_2})$$

where A and B are constants and $p(\infty)$ is the steady-state response of $p(t)$. However, for depolarizations to −50 and −40 mV, where I_{Na} inactivation approaches completion, $p(\infty) \to 0$, and the time constants (τ_{c_1}, τ_{c_2}) can be obtained from a simple semilogarithmic plot of $p(t)$ against time. Using the results shown in the Figure, τ_{c_1} was calculated as 0·7 msec and τ_{c_2} as 5·5 msec.

to −30 mV (Fig. 11*A*). When prepulses were used at potentials positive to the holding potential of −80 mV, onset of inactivation was measured, whereas hyperpolarizing pulses represent recovery from inactivation. At each prepulse potential, plots were constructed of the ratio of test pulse current with prepulse to that without, as a function of prepulse duration (Fig. 11*B*). For depolarizing prepulses to −40, −50

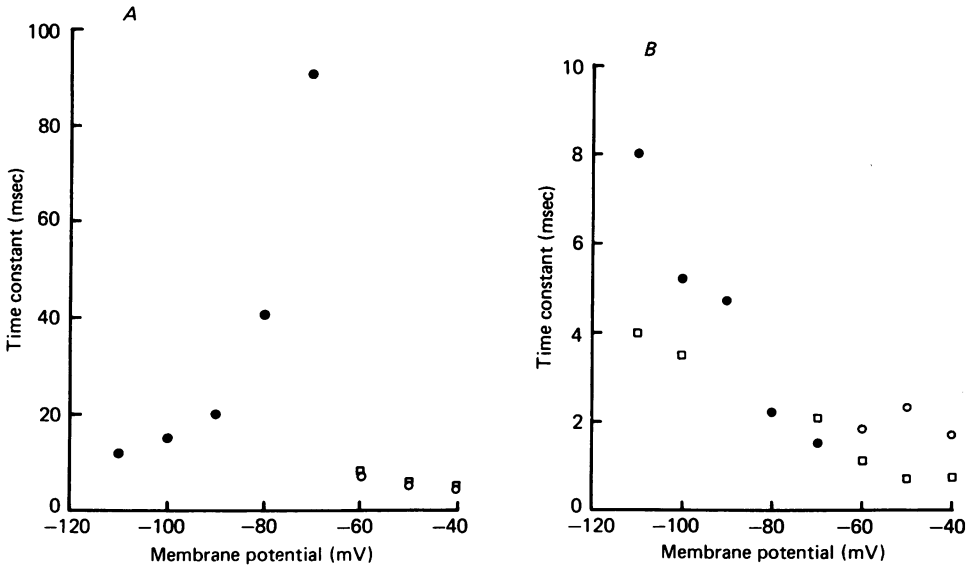

Fig. 12. Relationship between membrane potential and I_{Na} inactivation time constants in the potential range −40 to −110 mV. τ_{h_1}, τ_{h_2} values (○) obtained from single depolarizing pulses (Fig. 1*A*); τ_{c_1}, τ_{c_2} (□) using variable duration prepulses with a test pulse (Fig. 11*A*); τ_{r_1}, τ_{r_2} (●) with pre- and test-pulses separated by an interval of increasing duration (Fig. 9*A*). Data for mean values of τ_{h_2}, τ_{c_2} and τ_{r_2} shown in *A* and for τ_{h_1}, τ_{c_1}, τ_{r_1} in *B*; note change in ordinate scale between *A* and *B*.

or −60 mV, the curves could be fitted by two exponentials (Fig. 11*C*) having time constants τ_{c_1} and τ_{c_2}, which were similar in magnitude to the τ_{h_1} and τ_{h_2} values obtained from maintained depolarizations (Fig. 7 and Table 2). When more negative prepulses were used, only one time constant was found (τ_{c_1}), having the same magnitude as τ_{r_1} at the relative potential. The absence of a second time constant over the more negative potential range is due probably to the fact that prepulses were used only to a maximum duration of 8 msec, precluding detection of the slower component.

Fig. 12 shows the potential dependence of the mean values for inactivation time constants obtained with the three pulse protocols described above (Fig. 1*A*, 9*A* and 11*A*), over the range −40 to −110 mV. As described above, there were no values for τ_{c_2} at potentials more negative than −60 mV, precluding comparison with the τ_{r_2} values obtained. The faster components τ_{r_1}, τ_{c_1} and τ_{h_1} showed an increase from −40 to −110 mV (Fig. 12*B*), with less scatter between values at potentials positive to −70 mV.

Effect of TTX on the cardiac Na current

We find that I_{Na} in single cardiac myocytes is not as highly sensitive to TTX as I_{Na} in nerve or skeletal muscle. The Na current is not affected by TTX at doses below 3×10^{-8} M, but above this concentration gradual inhibition occurs. Half-maximal inhibition dosage occurred at 6×10^{-6} M and complete blockage occurred at 3×10^{-5} M. Both inactivation processes are blocked by TTX and there did not appear

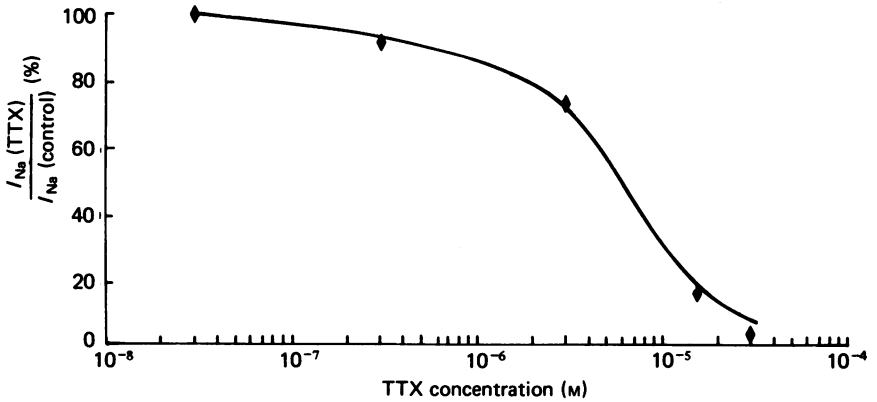

Fig. 13. Dose–response relationship between I_{Na} and TTX. TTX has no effect at 10^{-8} M and blocks completely at about 3×10^{-5} M. The over-all dose–response curve was sigmoidal and half-maximal inhibition concentration was $6{\cdot}0 \times 10^{-6}$ M. The continuous line was computed from

$$I_{Na}\,(TTX) = I_{Na}\,(control)\left\{1 - \left[\frac{1}{1+(K_M/[TTX])}\right]\right\}$$

where K_M is the dissociation constant of TTX. K_M was calculated to be 5×10^{-6} M. I_{Na} (TTX) is inward Na current in the presence of TTX. I_{Na} (control) represents Na current without TTX (control).

to be any difference in sensitivity. The over-all dose–response curve of the Na current to TTX concentration is sigmoidal and is shown in Fig. 13. The curve could be fitted to the equation

$$I_{Na}\,(TTX) = I_{Na\ (control)}\left(1 - \frac{1}{1+(K_m/[TTX])}\right)$$

where K_m is the dissociation constant of TTX. K_m is calculated to be about 5×10^{-6} M at a membrane potential of -30 mV.

DISCUSSION

The major finding of this study is that rapid inward Na current, elicited in individual myocardial cells at 20–22 °C by step depolarization under voltage clamp, can be separated temporally from capacitative current that appears as a brief ($\sim$ 100 μsec) discontinuity between the onset of the voltage-clamp step and activation of the ionic current. Further, clear resolution of capacitative and ionic currents not only revealed the activation phase of I_{Na} at all potentials tested, but also showed

transient outward I_{Na} at potentials positive to the Na equilibrium potential (Fig. 1 *B*). Outward Na currents elicited by step depolarizations have not been demonstrated previously in high Na solutions, due to obscuring capacity currents, although their presence was reported by Dudel, Peper, Rudel & Trautwein (1966) in Purkinje fibres bathed with low-Na solutions.

Since the instantaneous *I–V* relationship for I_{Na} was linear over the range of potentials employed, a Hodgkin–Huxley chord conductance model was used to calculate Na conductance, g_{Na} (Hodgkin & Huxley, 1952*a–d*). g_{Na} increased gradually as potentials became positive from −60 mV (Fig. 5) and $\bar{g}_{Na}$ was calculated to be about 25 mS cm^{-2}, assuming a cell surface area of 8000 μm^2. This value is lower than the 40–60 mS cm^{-2} reported by Dudel & Rudel (1970) for sheep Purkinje fibres cooled to 4 °C, but their result may be an over-estimation of $\bar{g}_{Na}$, since it was based on the external cylindrical surface area of their preparations (Noble, 1975). Assuming that the external surface area in a multicellular Purkinje fibre preparation represents only 10 % of the membrane area when deep cells are accounted for (Mobley & Page, 1972), then $\bar{g}_{Na}$ becomes 5–6 mS cm^{-2} at 4 °C. Even using Moore's (1958) correction (for squid giant axon) that $\bar{g}_{Na}$ increases 4 % per °C temperature rise, will only bring this value to about 40 % of the magnitude found in the present experiments for individual rat ventricular muscle cells. It is clear, however, that $\bar{g}_{Na}$ in heart muscle is smaller than the 120 mS cm^{-2} reported for squid giant axon by Hodgkin & Huxley (1952*d*).

Although cardiac I_{Na} is a smooth, uninterrupted function of membrane potential (Fig. 1 and 2), the kinetics reported here are rather more complex than those found for squid giant axon. The observation found consistently in this study that I_{Na} turns on after an initial delay is consistent with the delay in Na activation in squid axon (Hodgkin & Huxley, 1952*b*; Bezanilla & Armstrong, 1977), but the activation phase can be fitted by a Hodgkin–Huxley conductance model using an m^4 as well as an m^3 fit. Inactivation of I_{Na} appears to involve two time constants, one being at least three to four times as long as the other at all potentials tested. This biphasic nature of I_{Na} inactivation is not due to series resistance effects, since it was observed in solutions having reduced Na or containing low concentrations of TTX. It was also present at small depolarizing potentials, where series resistance effects, had they been significant, would have tended to accelerate the slower process (Meves, 1978). When only one suction pipette was used and series resistance effects were expected to be serious (Brown *et al.* 1981), I_{Na} relaxed in a monoexponential fashion. Further, the double exponential inactivation is not artifactual due to a non-linear leakage current, since leakage currents are small and linear over the clamp potential range used in the present experiments (Brown *et al.* 1981, Fig. 12). That these data require I_{Na} to be described by a Hodgkin–Huxley model with incomplete inactivation, or two inactivation time constants, is not a novel approach, for both Deck & Trautwein (1964) and McAllister & Nobel (1966) found a slow and incomplete inactivation of g_{Na} in Purkinje fibres, a result not confirmed by Dudel *et al.* (1966), Colatsky (1980) or Ebihara, Shigeto, Lieberman & Johnson (1980), but consistent with the results reported by Reuter (1968). The data presented here is the first description of a multi-exponential inactivation process in ventricular myocardium.

Values for I_{Na} inactivation time constant (τ_h) calculated using the computer algorithm, assuming a simple Hodgkin–Huxley formalism with incomplete inactiv-

ation, indicated that τ_h at -40 mV was three times longer than the corresponding value at 0 mV (Table 1). This was encouraging, since it is in complete agreement with the data reported by Hodgkin & Huxley (1952*d*) for squid giant axon, but the observation that the decay of I_{Na} under a maintained depolarization exhibits two time constants is direct evidence for second order properties of the inactivation system. The three-state inactivation model of Chiu (1977) was chosen for use in this paper solely on the grounds that it was a simple modification of the Hodgkin–Huxley formulation, which did predict two rate constants for every inactivation response. It must be emphasized that although the data reported here are consistent with this prediction, as onset of or recovery from inactivation can be described by double exponential functions, the question of the specific model required for describing I_{Na} inactivation and recovery in rat ventricular myocardium must remain open. In particular, the model formulated by Chiu (1977) predicts that the h_∞–V curve is best fitted by a function involving the sum of two exponentials, whereas we found that our data could be fitted by the simpler function proposed by Hodgkin & Huxley (1952*c*). However, the error bars associated with our h_∞–V curve (Fig. 8*A*) prevent detailed examination of this point, and the absence of a complete comparison of the results of this study with the Chiu model can be ascribed to the paucity of our data in certain respects. Thus, the recovery and onset experiments for I_{Na} inactivation were too time-consuming to be carried out on the same cell, and the prepulse duration for the τ_c experiments was too short to resolve the slow inactivation process at potentials near the normal resting membrane potential. Our data show clearly the biphasic nature of the inactivation processes taking place, but more comprehensive experimental results are required before a detailed consideration can be undertaken of either the Chiu model or other models, including those which couple I_{Na} activation with inactivation (Goldman, 1976; Meves, 1978).

The large values for τ_{r_2} found here for recovery from inactivation at potentials near the resting membrane potential are of the same order of magnitude as time constants reported previously. Haas *et al.* (1971) measured recovery time constants (τ_r) of 100 msec in frog atrial fibres, and Gettes & Reuter (1974) used $\dot{V}_{max}$ to show that τ_r is 10–20 msec at -90 to -80 mV, 50 msec at -70 mV and 125–150 msec at -60 mV. Gettes & Reuter (1974) observed long recovery time constants for I_{Na} inactivation in sheep, guinea-pig, pig and calf heart, and a similar finding was reported by Dudel & Rüdel (1970) for cooled Purkinje fibres. Colatsky (1980) has shown recently that τ_r in rabbit Purkinje fibres at 17–20 °C is of the order 170 msec in the potential range -70 to -90 mV (mean value for τ_r calculated from data in Table 3 of Colatsky, 1980).

The last distinguishing characteristic of cardiac I_{Na} observed in these single-cell studies was the low sensitivity to TTX, which was observed for as long as 48 hr after cell isolation, thus making the possibility of an inhibitory influence of the dissociation procedure unlikely. It is well known that blockade of I_{Na} in myocardium requires doses of TTX at 10^3–10^4 greater concentrations than in nerve or skeletal muscle (Narahashi, 1974) and observations similar to those presented here have been reported for guinea-pig papillary muscle (Baer, Best & Reuter, 1976) and Purkinje fibres (Dudel, Peper, Rüdel & Trautwein, 1967; Beeler & Reuter, 1970). We have not yet examined the possibility that the TTX effects may be voltage-dependent (Baer *et al.* 1976) or use-dependent (Cohen, Colatsky & Tsien, 1980).

Our results (Fig. 8*A* and *B*) also show a steady-state or 'window' Na current over a limited potential range, in agreement with the findings of Gadsby & Cranefield (1977) and Attwell, Cohen, Eisner, Ohba & Ojeda (1979). On the other hand, Ebihara *et al.* (1980), Colatsky & Tsien (1979) and Colatsky (1980) did not find any overlap of the m_∞^3 and h_∞ curves. These differences, together with the other discrepancies noted above, may reflect both differences in methodology and variations between preparations. Previous studies on Na currents in myocardium have been carried out on multicellular preparations, where the complex tissue structure limits the spatial and temporal control of the voltage-clamp method and allows concentration changes to occur in restricted extracellular spaces. In the present experiments there was good evidence of adequate voltage control (Brown *et al.* 1981), consistent with the observations that the envelope of I_{Na} tail currents show a double exponential time course similar to individual current–time records, and the relative constancy of *I–V* profiles over a large range of I_{Na} (Fig. 2). There was also good correlation between $\dot{V}_{max}$ (200–300 V sec^{-1}) and $\bar{g}_{Na}$ (25 mS cm^{-2}).

Another complicating factor in multicellular preparations is that suppression of other ionic currents, such as those carried by K and Ca, may not have been complete. For example, Ebihara *et al.* (1980) observed a slow inward current that was suppressed by the organic Ca channel blocker D-600, and Purkinje fibres have a fast outward K current with kinetics similar to those for I_{Na} (Kenyon & Gibbon, 1977; Siegelbaum & Tsien, 1980). The presence of such currents will obviously complicate kinetic measurements. In the experiments reported here, single cells were used to eliminate both the complex structure of whole tissue and ion accumulation or depletion in intercellular clefts. Furthermore, internal perfusion allowed removal and substitution of internal K with Cs ions, which permeate K channels poorly, if at all, and Ca currents were absent, since extracellular Ca was either omitted or substituted by Mn. Also, the replacement of Cl^- with the relatively impermeable aspartate and isethionate ions probably reduced shunt currents. It is likely, therefore, that the Na currents recorded in the present experiments were not contaminated significantly by other components, a contention supported by the observations that the reversal potential for I_{Na} varied with external Na in a manner predicted by the Nernst equation (Fig. 3) and that I_{Na} was blocked in a dose-dependent manner by TTX (Figs. 2 and 13).

On the other hand, it must be conceded that enzymic dispersion techniques may also introduce complications. The evidence presented here and elsewhere (Powell *et al.* 1980) that the passive electrical properties of single dispersed cells are similar to those found for whole tissue preparations, and that the measured Na currents are of sufficient magnitude to discharge the membrane capacitance at rates comparable to those found experimentally in both isolated cells and whole tissue preparations, would suggest that the effects of enzymic dissociation are not too severe.

This work was supported by N.I.H. grants HL-25145 and NS-11453 and the British Heart Foundation. It was done as a partial fulfilment of Kai S. Lee's doctoral thesis.

REFERENCES

ATTWELL, D., COHEN, I., EISNER, D., OHBA, M. & OJEDA, C. (1979). The steady state TTX-sensitive ('window') sodium current in cardiac Purkinje fibers. *Pflügers Arch.* **379**, 137–142.

BAER, M., BEST, P. M. & REUTER, H. (1976). Voltage-dependent action of tetrodotoxin in mammalian cardiac muscle. *Nature, Lond.* **263**, 344–345.

BEELER, G. W., JR. & REUTER, H. (1970). Voltage clamp experiments on ventricular myocardial fibres. *J. Physiol.* **207**, 165–190.

BEZANILLA, F. & ARMSTRONG, C. M. (1977). Inactivation of the sodium channel. I. Sodium current experiments. *J. gen. Physiol.* **70**, 549–566.

BROWN, A. M., LEE, K. S. & POWELL, T. (1980). Reactivation of the sodium conductance in single heart muscle cells. *J. Physiol.* **301**, 78–79*P*.

BROWN, A. M., LEE, K. S. & POWELL, T. (1981). Voltage clamp and internal perfusion of single rat heart muscle cells. *J. Physiol.* **318**, 455–477.

CHIU, S. Y. (1977). Inactivation of sodium channels: second order kinetics in myelinated nerve. *J. Physiol.* **273**, 573–596.

COHEN, C. J., COLATSKY, T. J. & TSIEN, R. W. (1980). Tetrodotoxin block of cardiac sodium channels during repetitive or steady depolarizations in the rabbit. *J. Physiol.* **296**, 70*P*.

COLATSKY, T. J. & TSIEN, R. W. (1979). Sodium currents in rabbit Purkinje fibre. *Nature, Lond.* **278**, 265–268.

COLATSKY, T. J. (1980). Voltage clamp measurements of sodium channel properties in rabbit cardiac Purkinje fibres. *J. Physiol.* **305**, 215–234.

COLQUHOUN, D. (1971). *Lectures on Biostatistics – an Introduction to Statistics with Applications in Biology and Medicine.* Oxford: Clarendon Press.

DECK, K. A. & TRAUTWEIN, W. (1964). Ionic currents in cardiac excitation. *Pflügers Arch.* **280**, 65–80. *Physiol.* **280**, 65–80.

DUDEL, J., PEPER, K., RÜDEL, R. & TRAUTWEIN, W. (1966). Excitatory membrane current in heart muscle (Pukinje fibers). *Pflügers Arch.* **192**, 255–273.

DUDEL, J., PEPER, K., RÜDEL, R. & TRAUTWEIN, W. (1967). The effect of tetrodotoxin on the membrane current in cardiac muscle (Purkinje fibers). *Pflügers Arch.* **295**, 213–226.

DUDEL, J. & RÜDEL, R. (1970). Voltage and time dependence of excitatory sodium current in cooled sheep Purkinje fibers. *Pflügers Arch.* **315**, 136–158.

EBIHARA, L., SHIGETO, N., LIEBERMAN, M. & JOHNSON, E. A. (1980). The initial inward current in spherical clusters of chick embryonic heart cells. *J. gen Physiol.* **75**, 437–456.

GADSBY, D. C. & CRANEFIELD, P. (1977). Two levels of resting potential in cardiac Purkinje fibers. *J. gen. Physiol.* **70**, 725–746.

GETTES, L. S., & REUTER, H. (1974). Slow recovery from inactivation of inward currents in mammalian myocardial fibres. *J. Physiol.* **240**, 703–724.

GOLDMAN, L. (1976). Kinetics of channel gating in excitable membrane. *Rev. Biophys.* **9**, 491–526.

HASS, H. G., KERN, R., EINWACHTER, H. M. & TARR, N. (1971). Kinetics of Na inactivation in frog atria. *Pflügers Arch.* **323**, 141–157.

HODGKIN, A. L. & HUXLEY, A. F. (1952*a*). Currents carried by sodium and potassium ions through the membrane of the giant axon of *Loligo*. *J. Physiol.* **116**, 449–472.

HODGKIN, A. L. & HUXLEY, A. F. (1952*b*). The components of membrane conductance in the giant axon of *Loligo*. *J. Physiol.* **116**, 473–496.

HODGKIN, A. L. & HUXLEY, A. F. (1952*c*). The dual effect of membrane potential on sodium conductance in the giant axon of *Loligo*. *J. Physiol.* **116**, 497–506.

HODGKIN, A. L. & HUXLEY, A. F. (1952*d*). A quantitative description of membrane current and its application to conduction and excitation in nerve. *J. Physiol.* **117**, 500–544.

KENYON, J. L. & GIBBONS, W. R. (1977). Effects of low chloride solutions on action potentials of sheep cardiac Purkinje fibers. *J. gen. Physiol.* **70**, 635–660.

LEE, K. S., WEEKS, T. A., KAO, R. L., AKAIKE, N. & BROWN, A. M. (1979). Sodium current in single heart muscle cells. *Nature, Lond.* **278**, 269–271.

LEE, K. S., AKAIKE, N. & BROWN, A. M. (1977). Trypsin inhibits the action of tetrodotoxin in neurones. *Nature, Lond.* **265**, 751–753.

LEE, K. S., AKAIKE, N. & BROWN, A. M. (1978). Properties of internally perfused, voltage-clamped isolated nerve cell bodies. *J. gen. Physiol.* **71**, 489–507.

MARQUARDT, D. W. (1963). An algorithm for least-square estimation of non-linear parameters. *J. ind. appl. Math.* **11**, 431–441.

MCALLISTER, R. E. & NOBLE, D. (1966). The time and voltage dependence of the slow outward current in cardiac Purkinje fibres. *J. Physiol.* **186**, 632–662.

MEVES, H. (1978). Inactivation of the sodium permeability in squid giant nerve fibers. *Prog. Biophys. molec. Biol.* **33**, 207–230.

MOBLEY, B. A. & PAGE, E. (1972). The surface area of sheep cardiac Purkinje fibres. *J. Physiol.* **220**, 547–563.

MOORE, J. W. (1958). Temperature and drug effects on squid axon membrane ion conductances. *Fedn. Proc.* **17**, 113.

NARAHASHI, T. (1974). Chemicals as tools in the study of excitable membranes. *Physiol. Rev.* **54**, 813–887.

NOBLE, D. (1975). *The Initiation of the Heartbeat.* pp. 48–52. Oxford: Clarendon Press.

POWELL, T., TERRAR, D. A. & TWIST, V. W. (1980). Electrical properties of individual cells isolated from adult rat ventricular myocardium. *J. Physiol.* **302**, 131–153.

SIEGELBAUM, S. A. & TSIEN, R. W. (1980). Calcium-activated transient outward current in calf cardiac Purkinje fibres. *J. Physiol.* **299**, 1–22.

WEIDMANN, S. (1970). Electrical constants of trabecular muscle from mammalian heart. *J. Physiol.* **210**, 1041–1054.